Electronic structure, magnetic, and cohesive properties of $Li_xMn_2O_4$: Theory

G. E. Grechnev,[1,2] R. Ahuja,[1] B. Johansson,[1,3] and O. Eriksson[1]
[1]*Department of Physics, University of Uppsala, Box 534, S-75121 Uppsala, Sweden*
[2]*Institute for Low Temperature Physics and Engineering, Kharkov 61103, Ukraine*
[3]*Department of Materials Science and Engineering, the Royal Institute of Technology, S-10044 Stockholm, Sweden*
(Received 11 June 2001; revised manuscript received 21 November 2001; published 19 April 2002)

The volume dependent electronic structure of the spinel-type lithium manganese oxides $Li_xMn_2O_4$, $x=0,0.5,1$, is studied *ab initio* by employing a full-potential electronic structure method. The electronic structure, total energies, open-circuit voltage, and magnetic moments were obtained for various spin configurations of $Li_xMn_2O_4$ in the cubic spinel structure and the low-temperature orthorhombic structure. The effect of magnetic ordering on the band structure and structural stability has been investigated and an antiferromagnetic ordering proved to be the ground state of the $Li_xMn_2O_4$ spinels. Our calculations show that the manganese majority t_{2g} d band is filled for all $Li_xMn_2O_4$ compounds studied, and the filling of the minority t_{2g} band is expected in the lithiation process. The lithium intercalation potential, bulk modulus, magnetic moments, and optical properties are calculated within the itinerant band approach and are found to be in good agreement with available experimental data, indicating, that the density-functional theory provides reliable electronic structure of the $Li_xMn_2O_4$ system. The effect of the orthorhombic distortion on electronic structure and magnetism of $LiMn_2O_4$ was investigated, and our calculations do not show a substantial charge ordering at the structural transition from the cubic spinel to the orthorhombic structure, as proposed earlier. Instead, the low-temperature orthorhombic structure is found to possess the lowest energy via a Jahn-Teller distortion driven by the d band.

DOI: 10.1103/PhysRevB.65.174408 PACS number(s): 71.20.Ps, 61.66.Fn, 84.60.Dn

I. INTRODUCTION

In the recent years a considerable interest in lithium manganese oxides $Li_xMn_2O_4$, $0\leqslant x\leqslant 2$, has developed due to their application potential as rechargeable battery electrodes (e.g., Refs. 1 and 2). The cubic spinel oxides derive their properties from the large stability region they have with respect to the lithium content. The lithium content x can be varied between 0 and 1 and even higher without substantial changes in the spinel structure of these oxides. This Li-intercalation mechanism is the basis for its application as an electrode in a rechargeable battery.

Whereas numerous experimental investigations were devoted to electrochemical characteristics of the lithium cells, the more recent[3–21] studies were aimed to investigate structural, electronic, magnetic, and optical properties of the spinel-type lithium manganese oxides. Various structural and magnetic phase transitions were observed in the $Li_xMn_2O_4$ system.[3,4,6,10,12–14] The structural phase transitions are believed to be caused by the cooperative Jahn-Teller distortions, associated with Mn^{3+} ions.[1,2,22] In particular, the $LiMn_2O_4$ compound, with the average manganese valence $+3.5$, is regarded as having an equal number of randomly distributed Mn^{+4} and Mn^{3+} ions above room temperature. Though in the cubic spinel phase all manganese sites are equivalent, the high spin Mn^{3+} ions favor dynamic Jahn-Teller distortions, which are presumably responsible for the structural phase transition at temperatures $T_V\simeq 285$ K, accompanied by a corresponding charge ordering. This transition is believed to be analogous to the Verwey transition in magnetite, Fe_3O_4.[22,23]

A problem with the commercial use of $LiMn_2O_4$ spinel is related to the corresponding lattice instability, and a great deal of effort is going into the investigation of the nature of this phase transition,[3–6,10,12–15,19–21] which remains disputable. It is still not clear whether the low-temperature (below $T_V\simeq 285$ K) phase of $LiMn_2O_4$ is orthorhombic[13,14] or tetragonal.[10] Also, according to the recent studies,[10,19] the phase transition does not lead to a total transformation of the spinel structure until a temperature of 70 K has been reached, and only partial segregation of Mn^{+4} and Mn^{3+} ions was found. A hopping of Li ions between two crystallographically different sites, $8a$ and $16c$, was recently observed in the spinel phase at temperatures above the phase transition.[8,21] This hopping is presumably not favorable for the charge ordering of Mn^{3+} and Mn^{4+}. Moreover, with the small substitution of manganese by lithium on $16d$ sites in $Li(Mn_{1.96}Li_{0.04})O_4$, no Jahn–Teller distortions were found in the temperature range 4–290 K by means of the neutron diffraction.[20] This indicates that different mechanisms, such as the lithium intersite hopping,[8,21] $(8a)\rightarrow(16c)$, or substitution of manganese by lithium,[20] $(8a)\rightarrow(16d)$, as well as competing magnetic interactions,[10] have to be taken into account to elucidate a nature of the phase transition in the $LiMn_2O_4$ spinel at 285 K.

Geometrical frustration of the antiferromagnetic ordering in the pyrochlore network in the spinel structure, combined with mixed-valent distribution of Mn ions, are presumably responsible for the complex magnetic structure expected in $LiMn_2O_4$.[10,15] Spin-glass-like behavior was reported[16,17] in $LiMn_2O_4$ at low temperatures, whereas a long-range-ordered complex antiferromagnetic state with 1152 magnetic Mn ions was proposed in Ref. 10. Therefore, theoretical studies of the electronic structure, ground-state, and excited-state properties are necessary to understand the complex physical nature

of the $Li_xMn_2O_4$ system and to analyze a wealth of experimental data.

Theoretical investigations have previously been carried out to reveal basic features of the electronic structure for the lithiated manganese oxides by means of DV-Xα molecular orbital,[24] linear-muffin-tin orbital (LMTO-ASA),[25] full potential (FP) LAPW,[26] and pseudopotential[27–29] calculations. The most comprehensive *ab initio* calculations were performed in Ref. 26 (for the layered manganese oxides) and in Refs. 27–29, where spin-polarization effects were taken into account within FP-LAPW and VASP pseudopotential techniques, respectively. It was argued[28] that stabilities of spin-polarized spinel phases of Mn_2O_4 and $LiMn_2O_4$ can be described within density-functional theory (DFT), moreover the generalized gradient approximation[30] (GGA) has provided somewhat better agreement with experiment than the local-spin-density approximation[31] (LSDA).

The *ab initio* electronic structure calculations for mixed-valent manganese oxides represent a challenge to the density-functional theory. In $Li_xMn_2O_4$ compounds the dynamical Jahn–Teller distortions at randomly distributed Mn^{3+} ions are accompanied by hopping of Li ions between 8*a* and 16*c* sites,[8,21] which can cause the transferred hyperfine coupling between Mn and Li spins.[7,21] Also, it is extremely difficult to find a ground state of frustrated antiferromagnetic structure among a large number of degenerate noncollinear spin configurations. In this connection, the prime objective of the present work is to elucidate the electronic structure of $Li_xMn_2O_4$ spinels, specifically for both systems in the vicinity of the expected Verwey transition, including the low-temperature complex orthorhombic structure of $LiMn_2O_4$, by taking into account spin polarization in a feasible, simplified form. The related bulk, magnetic, and optical properties of these manganese oxides were evaluated and analyzed in order to reveal possible manifestations of spin, structural, and charge ordering in the framework of the density-functional theory. The results of *ab initio* calculations can also be helpful in revealing trends favorable for a suppression of Jahn-Teller distortions, which are responsible for the limited cycle lifetime and capacity loss in the $LiMn_2O_4$ batteries.

II. STRUCTURAL DETAILS AND COMPUTATIONAL TECHNIQUE

The cubic spinel $LiMn_2O_4$ has a face-centred Bravais lattice (space group $Fd\bar{3}m$ or O_h^7, comprising 2 f.u. in the fcc unit cell), where the Li atoms occupy one-eighth of the tetrahedral (8*a*) sites, and the Mn atoms occupy half of the octahedral (16*d*) sites in an intervening cubic closed-packed formation of oxygen atoms (at 32*e* sites). For a lithium concentration $x=0.5$, $Li_{0.5}Mn_2O_4$, we assumed an ordered arrangement of Li, i.e. one of two lithium sites in the $LiMn_2O_4$ cell is filled, another one is empty. The experimental values of the internal oxygen parameter *u* were fixed in our calculations, with the lattice parameter *a* varying in a wide range for the $Li_xMn_2O_4$ compounds studied.

The delithiated phase of $Li_xMn_2O_4$ spinels, which actually contains a small residual amount of lithium ($Li_{0.06}Mn_2O_4$, Ref. 9), is called λ-MnO_2. It represents one of the metastable forms of manganese dioxides and results from electrochemical removal of lithium from $LiMn_2O_4$ cathodes in the battery cell within the charge cycling process. This compound retains the basic $Fd\bar{3}m$ structure with some lower lattice parameter *a*, compared to $LiMn_2O_4$, and with lithium atoms removed from the spinel framework.

Below the Verwey-like transition at $T_V \simeq 285$ K, the complex orthorhombic phase of $LiMn_2O_4$ (space group $Fddd$) was established in Refs. 13 and 14. It can be viewed as a distorted cubic spinel structure with a tripled periodicity in two directions, a "$3a\times 3a\times a$" cell, where *a* is approximately equal to a lattice parameter of the cubic spinel structure. The structural optimization has not been performed for this orthorhombic phase due to complexity of the structure, and all structural parameters used in the calculations are taken from Ref. 13. The accepted orthorhombic structure is actually very close to a large tetragonal cell (space group $I4_1/amd$), which was also proposed in Ref. 10 for the low-temperature phase of $LiMn_2O_4$.

Ab initio calculations of the electronic structures were performed for $Li_xMn_2O_4$ oxides, $x=0,0.5,1$, by employing a full-potential LMTO method[32] (FP-LMTO). In this all-electron method the Kohn-Sham equations can be solved without any shape approximations imposed on the charge density or potential. An elementary cell is subdivided into MT spheres at atomic sites and an interstitial part. Inside the MT spheres the basis functions, charge density, and potential are expanded in spherical harmonic functions multiplied by a radial function, whereas in the interstitial region charge density and potential are expanded in a Fourier series. A basis function in the interstitial part is a Bloch sum of Neumann and Henkel functions, which are augmented by numerical basis function inside MT spheres. The spherical-harmonic expansion of the charge density, potential and basis functions were carried out up to a cutoff in angular momentum $l=6$. The tails of the basis functions outside their parent spheres are linear combinations of Hankel or Neumann functions depending on the sign of the kinetic energy of the basis function in the interstitial region. Further, a so-called "double basis" has been adopted, where two different orbitals for the same principal and angular quantum number are connected at the sphere boundaries, in a continuous and differentiable way, to Hankel or Neuman functions with different kinetic energies in the interstitial region. In the present calculations the basis set included *s*, *p*, and *d* orbitals for valence states of all constituents, including lithium and oxygen.

The exchange-correlation potential was treated in both the LSDA (Ref. 31) and GGA (Ref. 30) of the density-functional theory. For the core charge density, the Dirac equation is solved self-consistently, i.e., no frozen core approximation was used. The effect of the spin-orbit coupling, included in the Hamiltonian, appeared to be almost negligible for the calculated electronic structure of $Li_xMn_2O_4$, and most of the present calculations were carried out in the scalar-relativistic approximation. The integration over the Brillouin zone in the self-consistency cycle was performed using the special point sampling[33] with around 60 **k** points for the cubic spin-

TABLE I. The bulk, electronic, and magnetic properties of $Li_xMn_2O_4$ spinels, calculated in the local-spin-density approximation and the general-gradient approximation. Lattice parameters a are given in Å. Bulk moduli B are in GPa. The average intercalation voltages $\overline{V}$ are in eV. The total energies ΔE, in eV/f.u., are defined with respect to the corresponding nonmagnetic spinel. The density of states at the Fermi level, $N(E_F)$, is in states/(eV f.u.). The magnetic moment within the Mn MT sphere, M_{Mn}, is in μ_B.

		a (Å)		B (GPa)		$\overline{V}$ (eV)		M_{Mn} (μ_B)		ΔE_{sp} (eV)		$N(E_F)$ (eV^{-1})	
Spinel	Phase	LSDA	GGA	LSDA	GGA	LSDA	GGA	LSDA	GGA	LSDA	GGA	LSDA	GGA
λ-Mn_2O_4	NM	7.90	8.02	221	194					0	0	7.5	7.3
	FM	7.95	8.16	204	179			2.78	2.79	−1.38	−1.40	0	0
	AFM	7.94	8.14	206	180			2.77	2.78	−1.45	−1.48	0	0
	Expt.		8.04[a]						2.8[b,c]				
$Li_{0.5}Mn_2O_4$	NM	7.96	8.00	214	199	2.1	2.1			0	0	7.7	7.4
	FM	8.01	8.14	208	185	2.3	2.2	2.63	2.65	−1.43	−1.45	0	0
	Expt.		8.14[a]				3.6[a]						
$LiMn_2O_4$	NM	8.03	7.99	212	199	3.7	3.8			0	0	7.3	6.9
	FM	8.08	8.13	204	181	3.9	3.9	2.48	2.50	−1.51	−1.45	5.5	5.2
	AFM	8.09	8.12	205	182	3.9	3.8	2.48	2.49	−1.50	−1.48	6.9	6.6
	Expt.		8.23[a]		200[d]		4.1[a]		3.2[c]				

[a]Reference 8.
[b]Reference 9.
[c]Reference 17.
[d]Reference 3.

polarized configurations of $Li_xMn_2O_4$, and eight **k** points for the orthorhombic $LiMn_2O_4$ supercell. In this integration a Gaussian smearing was employed with the width of 20 mRy to accelerate the convergence. After achievement of self-consistency, the tetrahedron method was employed for the density of states (DOS) and optical calculations on a fine **k**-point grid.

The calculations were performed for the cubic spinel structure as well as the orthorhombic structure of $LiMn_2O_4$ for nonmagnetic (NM), ferromagnetic (FM), and antiferromagnetic (AFM) configurations. For the spinel $Li_xMn_2O_4$ systems in the AFM configuration two of the manganese atoms in the unit cell were chosen as having spins ''up,'' and the other two as ''down'' spins along the [001] direction. In the low-temperature orthorhombic structure of $LiMn_2O_4$, the assigned AFM configuration corresponds to alternating planes with ''up'' and ''down'' Mn moments. Using the calculated self-consistent potentials, the optical dielectric tensor was calculated for the PM, FM, and AFM cubic spinel phases of $LiMn_2O_4$ with the linear tetrahedron technique, as it was proposed in Refs. 32 and 34. The absorption coefficient $I(\omega)$ is proportional to the imaginary part of the extinction coefficient k times the frequency,

$$I = 2\omega k/c, \tag{1}$$

where c is the speed of light, and k can be evaluated by using the calculated real and imaginary parts of the dielectric tensor.[34] In order to reproduce experimental conditions, related to the finite lifetime of the excited states and the instrumental smearing, the calculated spectra were broadened.

III. RESULTS AND DISCUSSION

A. Equilibrium properties

In the framework of *ab initio* FP-LMTO calculations, the total energies E of $Li_xMn_2O_4$ spinels ($x=0,0.5,1$) were calculated as functions of volume V, and were then fitted to analytical parametrizations for the equation of state, such as the Murnaghan and recently proposed universal[35] equation of state, both have given almost identical $E(V)$ curves. The equilibrium lattice spacings and bulk moduli are evaluated from the corresponding equations of state, and are presented in Table I (LSDA and GGA results). The GGA provides lattice constants close to the experiment, and a bulk modulus of the antiferromagnetic phase, which is somewhat smaller than the LSDA experimental data. On the other hand, the LSDA calculated lattice parameters appeared to be consistently smaller (about 2%) than the experimental ones, although they reproduce the lattice expansion when the lithium concentration x increases from 0 to 1. In addition the LSDA bulk modulus is in better agreement with experiment than the GGA result. When comparing the LSDA and GGA results one comes to the conclusion that they are rather similar and that the LSDA data are in somewhat better agreement with experiment than GGA. The most obvious shortcoming of the GGA calculation is that the expansion of the lattice constant with increasing Li concentration is not reproduced. We remark that although GGA normally improves the equilibrium volumes of solid state matter compared to LDA, there are exceptions to this finding and the presently studied system is one more such example.

B. Open-circuit voltage

The calculations of the total energy can provide the average open-circuit voltage $\overline{V}$ (OCV) for the following reaction:

$$\mathrm{Li(anode)} + 2\mathrm{MnO_2(cathode)} \Rightarrow \mathrm{LiMn_2O_4(cathode)}. \quad (2)$$

The Li intercalation potential and the average OCV is given by[27]

$$\overline{V} = -\Delta G/F, \quad (3)$$

where ΔG is Gibbs' free energy for the intercalation reaction, and F is the Faraday constant. The energy of Li was calculated for the bcc structure of the metal. In the present work ΔG was approximated by the change in internal energy ΔE, whereas both the volume ($P\Delta V$) and the entropy ($T\Delta S$) contributions to ΔG were neglected, as has been proved to be sufficient in Ref. 27. The calculated lithium intercalation voltage is given in Table I (LSDA and GGA results), and both approximations result in an OCV that is in agreement with experiment for $LiMn_2O_4$. On discharging, a change in the OCV potential can be considerable[25] and not strictly fixed for the intermediate systems, e.g., $Li_{0.5}Mn_2O_4$. Therefore, the OCV calculated for the $Li_{0.5}Mn_2O_4$ system should, with caution, be compared with the corresponding experimental data.[8] Also, the lithium intersite hopping between 8*a* and 16*c* sites, which is presumably the primary lithium conduction process[21] in the $Li_xMn_2O_4$ spinels, can contribute to this discrepancy.

C. Electronic structure

As a whole, the electronic structure of $Li_xMn_2O_4$ compounds is governed by a strong hybridization between the Mn *d* and O *p* states, whereas lithium atoms are substantially ionized in these spinels. The lowest-lying states in both systems correspond mostly to the filled *p* states of oxygen. In $Li_xMn_2O_4$ spinels the Fermi level E_F lies within the nonbonding t_{2g} band, originating predominantly from the *d* states of manganese. Below E_F a strong hybridization of oxygen *p* states and *s*,*p*,*d* states of manganese gives rise to the filled Mn–O bonding bands. The e_g bands are found to be empty in all non-spin-polarized systems studied in the present work.

The total densities of electronic states, $N(E)$, calculated for the antiferromagnetic phases of $LiMn_2O_4$ in the cubic spinel and the low-temperature orthorhombic structures, are presented in Figs. 1 and 2, respectively. It includes the Mn majority spin t_{2g} *d* orbitals, which are filled for all spin-polarized $Li_xMn_2O_4$ compounds. For the delithiated λ-MnO_2 spinel an energy gap is found between the majority and minority t_{2g} bands. The lithiation process is accompanied by the filling of the weakly bonding minority t_{2g} band. This does not affect bulk properties noticeably, as can be seen from the calculated bulk moduli in Table I, and the moduli appeared to be in agreement with the experimental data available for $LiMn_2O_4$.[3]

The density of states at E_F in both spinel and orthorhombic $LiMn_2O_4$ systems comes essentially from the *d* electrons in MT spheres of Mn, and the partial contributions of other states are smaller at E_F [see Figs. 1(b–d)]. The conductivity in $LiMn_2O_4$ was interpreted in terms of hopping of small polarons, related to distortions at Mn^{+3} ions.[1,11,19] On the other hand, the thermoelectric power data were related[19] to

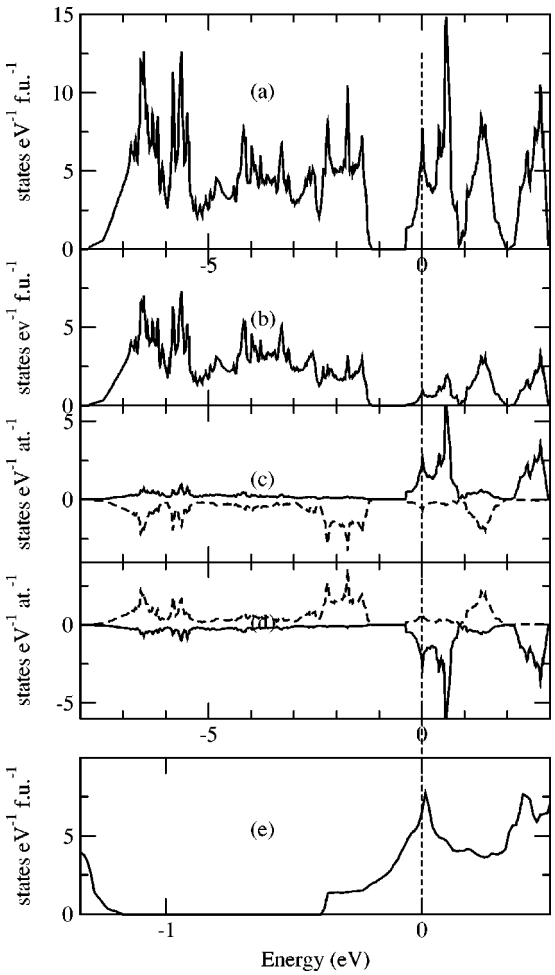

FIG. 1. Density of states $N(E)$ for the antiferromagnetic $LiMn_2O_4$ in the cubic spinel structure. The Fermi level is marked with a vertical dashed line. (a) The total DOS. (b) The contribution to the total DOS from the MT spheres of oxygen. (c) and (d): The contributions to the total DOS from the majority (dashed line) and minority (solid line) spin-polarized states of two Mn atoms with the opposite magnetic moments. (e) The finer structure of the total DOS at E_F. Note the different energy scales.

an assumed peak in $N(E)$ at E_F, which also results from the present calculations [see Figs. 1(a,e)]. The sharp peak of weakly bonding *d* states at E_F in the spinel AFM phase of $LiMn_2O_4$ implies the presence of a pronounced van Hove singularity in the electronic spectrum. This singularity can be related to a possible instability, and it can be seen in Fig. 2(b) that the orthorhombic (presumably Jahn-Teller driven) distortions produce a lowering of $N(E)$ at E_F. In line with this argument we found that the total energy of the orthorhombic phase is lower than that of the $LiMn_2O_4$ spinel (see Table II). A possible way to avoid this van Hove singularity at E_F is to alloy with elements that change the band filling, e.g., to replace some of the Mn ions with Cr or Fe. This may lead to avoidance of the structural transformation to the orthorhombic phase. Also, the recent experimental data obtained for $Li(Mn_{1.96}Li_{0.04})O_4$ alloys[20] could possibly be explained by this mechanism.

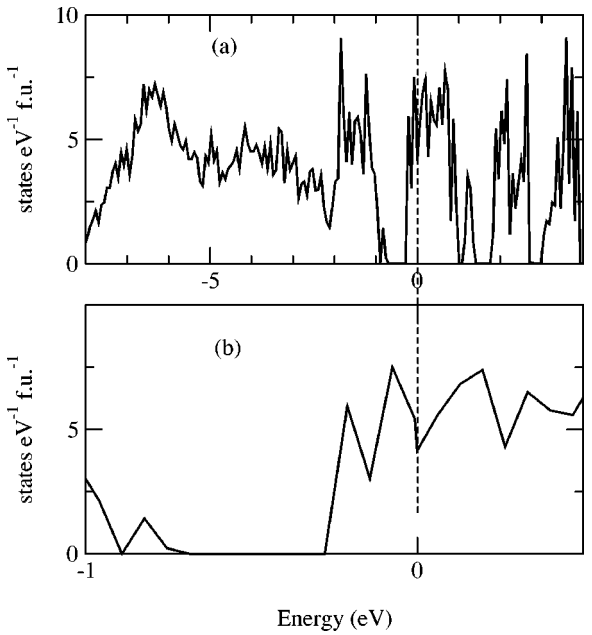

FIG. 2. Density of states $N(E)$ for the antiferromagnetic $LiMn_2O_4$ in the orthorhombic structure. The Fermi level is marked with a vertical dashed line. (a) The total DOS. (b) The finer structure of the total DOS at E_F. Note the different energy scales.

D. Spin and charge densities

As can be seen in Figs. 1 and 2, the distorted coordination octahedra in the orthorhombic phase give rise to wider gaps between t_{2g} and e_g bands, and the wider occupied bonding band. Next, we show the calculated charge density of the orthorhombic phase of $LiMn_2O_4$ for a cut in the (110) plane (Fig. 3). Although some difference in the charge-density distribution can be seen around different Mn ions due to the orthorhombic lattice distortions, it is much smaller than the pronounced charge ordering for Mn^{+3} and Mn^{+4} ions, which is expected for the Verwey-like transition[12,13] that was proposed as an explanation to the experiments in Ref. 13. The calculated spin density of the orthorhombic AFM $LiMn_2O_4$ for a cut in the (110) plane is shown in Fig. 4. The spin density originates primarily from the AFM ordered Mn atoms, and reflects the symmetry of the t_{2g} d electrons.

E. Magnetic moments

The antiferromagnetic phase was calculated to be a ground state of $LiMn_2O_4$, though the total energy of the ferromagnetic phase is only slightly higher, for both systems (spinel and orthorhombic, see Table II). The magnetic moments were calculated for the spin-polarized $Li_xMn_2O_4$ systems, and are presented in Tables I (LSDA and GGA) and II (GGA in the orthorhombic and spinel structure). Note that LSDA and GGA give similar magnetic moments. For the delithiated λ-MnO_2 spinel the calculated moment at the Mn site appeared to be in a good agreement with the experimental one evaluated from the neutron-diffraction measurements.[9] Unfortunately, there are no corresponding

TABLE II. The properties of $LiMn_2O_4$ in the spinel and the orthorhombic phases, calculated in the generalized-gradient approximation. Average magnetic moment within Mn MT sphere, M_{Mn}, is in μ_B. The total energies ΔE, in eV/f.u., are defined with respect to the nonmagnetic spinel total energy. The density of states at the Fermi level, $N(E_F)$, is in states/(eV f.u.).

Structure	Phase	M_{Mn} (μ_B)	ΔE (eV)	$N(E_F)$ (eV^{-1})
$LiMn_2O_4$	FM	2.50	−1.45	5.2
Spinel	AFM	2.49	−1.48	6.6
$LiMn_2O_4$	FM	2.27	−1.50	2.9
Orthorhombic	AFM	2.28	−1.53	4.2

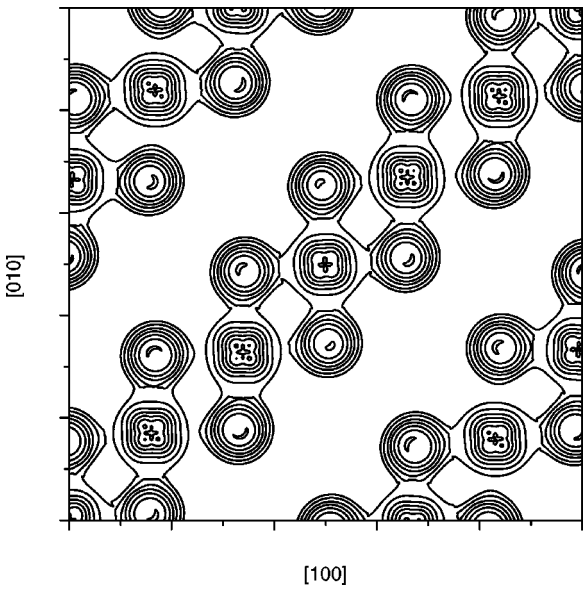

FIG. 3. Calculated charge density of the orthorhombic AFM $LiMn_2O_4$ for a cut in the (001) plane. The Mn atoms have a squared-like shape of the charge density, whereas O atoms are more spherically symmetric. No Li atoms are present in this plane.

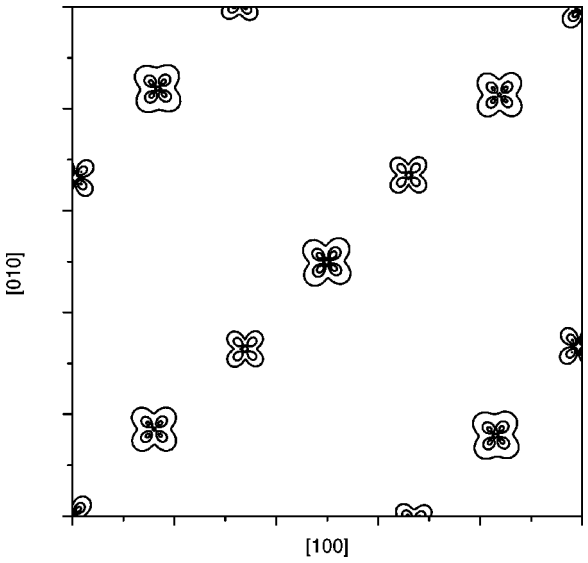

FIG. 4. Calculated spin density of the orthorhombic AFM $LiMn_2O_4$ for a cut in the (001) plane. The spin density originates primarily from the AFM ordered Mn atoms, and represents t_{2g} d electrons. When going along the [110] diagonal direction, every other atom has ''spin-up'' and ''spin-down'' density.

data available for $LiMn_2O_4$, though a number of neutron studies have been carried out on this system.[8,13,10,14,15] The magnetic unit cell of $LiMn_2O_4$ appeared to be very complex, estimated to contain at least 1152 magnetic atoms per cell.[10] The complexity of this frustrated antiferromagnetic structure is believed to be related[10,14,15] to the partial charge ordering at low temperatures and to a large number of metastable states available. It is consistent with the results of our spin-polarized calculations, which give very close total energies and magnetic moments for the FM and the AFM structures (see Tables I and II). We also observe in Table II that the calculated magnetic moment is quite sensitive to the crystalline structure.

A Curie-Weiss-like behavior was observed in the temperature dependence of the magnetic susceptibility χ for $Li_xMn_2O_4$ compounds.[3–5,9,10,17] In the paramagnetic temperature regime antiferromagnetic interactions appeared to be dominant, providing comparatively large and negative paramagnetic Curie temperatures, $|\Theta| \geqslant 100$ K.[17] The frustrated antiferromagnetic structure is presumably related to the suppression of the transition temperatures T_N with respect to the value of Θ,[10] as well as to deviations of $\chi^{-1}(T)$ from the Curie-Weiss (CW) behavior. These deviations, together with a possible variation in the composition of the samples, result in differing values of the Curie constants and Θ.[3–5,9,10,17] Since our fully relativistic calculations have provided small values of the orbital magnetic moments for Mn in $LiMn_2O_4$ and λ-MnO_2 (about $0.03\mu_B$), the Curie-Weiss effective moment was assumed to be dependent on the spin S only,

$$\mu_{\text{eff}} = \sqrt{4S(S+1)}. \tag{4}$$

Using the Curie constants obtained recently for λ-MnO_2 and $LiMn_2O_4$ in Ref. 17, the corresponding experimental CW spin moments were evaluated and presented in Table I. For the delithiated λ-MnO_2 spinel there is a good agreement between the calculated Mn moment and the spin moments evaluated either from the neutron studies[9] or from the CW analysis.[17] One should, however, remember that the CW moment does not always agree with the low-temperature saturation moment, and the comparison between theory and experiment is, on a formal level, best for the low-temperature moment. In the case of $LiMn_2O_4$ spinel, the CW spin moment appeared to be larger than the calculated one. However as pointed out above the comparison between CW moments and the low-temperature theory (or experiment) is not always straight forward. We conclude this section by noting that the $LiMn_2O_4$ spinel is probably not a well-behaved spin-only material. The deviations from the CW law were observed in the $\chi^{-1}(T)$ behavior,[3–5,9,10,17] and the apparent CW moment per Mn ion can vary considerably from the calculated spin-only value.

F. Optical data

In general, the DFT approach has obvious limitations in describing the excited electronic states. Nevertheless, in many cases the calculated optical spectra appear to be in agreement with experiment and provide a further insight into the electronic structure of complex oxides.[34] In the present work, the optical-absorption spectrum of the antiferromagnetic $LiMn_2O_4$ spinel has been calculated within the GGA. As can be seen in Fig. 5, there is a good agreement with the recent experimental data of Ref. 18. The features at the absorption coefficient $I(\omega)$ can be associated with transitions between the exchange and crystal-field split t_{2g} and e_g bands.

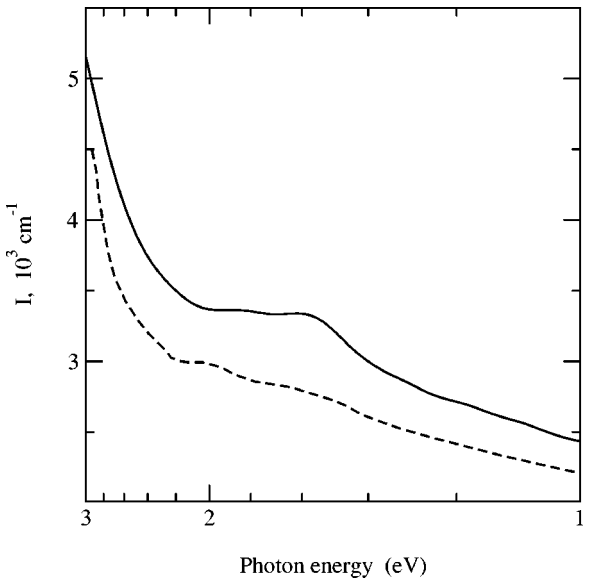

FIG. 5. The optical absorption coefficient $[I(\omega)]$ of $LiMn_2O_4$ in the cubic spinel phase. The solid line corresponds to the calculated spectrum for the AFM phase. The dashed line represents the experimental data of Ref. 18.

IV. CONCLUSIONS

The *ab initio* full-potential LMTO band-structure calculations have been performed for the spinel-type lithium manganese oxides $Li_xMn_2O_4$. Our calculations show that the spin polarization is essential to describe the basic properties of the $Li_xMn_2O_4$ oxides. The manganese majority t_{2g} d bands were found to be filled for all $Li_xMn_2O_4$ compounds studied, and the minority t_{2g} band was calculated to become filled in the lithiation process. The antiferromagnetic ordering is proved to be favorable as the ground state of $Li_xMn_2O_4$ spinels and the manganese e_g bands remains empty in all systems considered in the present work.

The distorted coordination octahedra in the orthorhombic phase of $LiMn_2O_4$ gives rise to wider gaps between t_{2g} and e_g bands. On the other hand, one can not exclude a possibility that for a true ground-state spin-polarized structure of $LiMn_2O_4$ (Ref. 10) the minority t_{2g} band can overlap with the majority e_g band. For the simplified AFM structures of $LiMn_2O_4$, our calculations have not produced a substantial charge ordering at the structural transition from the cubic spinel to the orthorhombic structure, in contradiction to the conclusion of Ref. 13. Instead, the transition seems to be driven by a Jahn-Teller-like distortion of the d band. Alloying with e.g. Fe would move the Fermi level away from the peak in the DOS that causes the Jahn–Teller effect, and the

structural phase transition may be avoided.

A number of ground-state properties, such as lithium intercalation potential, equilibrium volume, bulk modulus, and magnetic moments are calculated within the itinerant band approach and are found to be in good agreement with available experimental data, indicating that the density-functional theory describes the electronic structure of the $Li_xMn_2O_4$ system in a reliable way. The DFT calculations have also provided the optical absorption spectrum of $LiMn_2O_4$ in good agreement with experiment.

Manganese oxides are usually considered as strongly correlated systems, which presumably cannot be treated appropriately by DFT band theory. However, the present full-potential LMTO calculations, with GGA corrections included, described a number of ground- and excited-state properties observed in $Li_xMn_2O_4$ spinels. Finally, the present study supports the view that a strong coupling of the conduction electrons to a local Jahn-Teller distortion is important for understanding the kinetic properties of $Li_xMn_2O_4$ spinels, as well as the magnetic ordering in these compounds.

ACKNOWLEDGMENTS

This work was supported by The Swedish Natural Science Research Council (VR) and the Swedish Foundation for Strategic Research (SSF). We are grateful to Dr. J. Wills for supplying the FP-LMTO program.

[1] J. B. Goodenough, A. Manthiram, and B. Wnetrzewski, J. Power Sources **43-44**, 269 (1993).
[2] J. B. Goodenough, Solid State Ionics **69**, 184 (1994).
[3] J. Sugiyama, T. Tamura, and H. Yamauchi, J. Phys.: Condens. Matter **7**, 9755 (1995).
[4] J. Sugiyama, T. Hioki, S. Noda, and M. Kontani, J. Phys. Soc. Jpn. **66**, 1187 (1997).
[5] J. Sugiyama, T. Atsumi, A. Koiwai, T. Sasaki, T. Hioki, S. Noda, and N. Kamegashira, J. Phys.: Condens. Matter **9**, 1729 (1997).
[6] Y. Shimakawa, T. Numata, and J. Tabuchi, J. Solid State Chem. **138**, 138 (1997).
[7] P. Mustarelli, V. Massarotti, M. Bini, and D. Capsoni, Phys. Rev. B **55**, 12 018 (1997).
[8] H. Berg and J. O. Thomas, Solid State Ionics **126**, 227 (1999).
[9] J. E. Greedan, N. P. Raju, A. S. Wills, C. Morin, and S. M. Shaw, Chem. Mater. **10**, 3058 (1998).
[10] A. S. Wills, N. P. Raju, and J. E. Greedan, Chem. Mater. **11**, 1510 (1999).
[11] E. Iguchi, N. Nakamura, and A. Aoki, Philos. Mag. B **78**, 65 (1998).
[12] H. Yamaguchi, A. Yamada, and H. Uwe, Phys. Rev. B **58**, 8 (1998).
[13] J. Rodriguez-Carvajal, G. Rousse, C. Masquelier, and M. Hervieu, Phys. Rev. Lett. **81**, 4660 (1998).
[14] V. Massarotti, D. Capsoni, M. Bini, P. Scardi, M. Leoni, V. Baron, and H. Berg, J. Appl. Crystallogr. **32**, 1186 (1999).
[15] Y. Oohara, J. Sugiyama, and M. Kontani, J. Phys. Soc. Jpn. **68**, 242 (1999).
[16] Y. Jang, F. C. Chou, and Y.-M. Chiang, Appl. Phys. Lett. **74**, 2504 (1999).
[17] Y. Jang, B. Huang, F. C. Chou, D. R. Sadoway, and Y.-M. Chiang, J. Appl. Phys. **87**, 7382 (2000).
[18] K. Kushida and K. Kuriyama, Appl. Phys. Lett. **77**, 4154 (2000).
[19] J. Molenda, K. Swierczek, M. Molenda, and J. Marzec, Solid State Ionics **135**, 53 (2000).
[20] V. W. J. Verhoeven, F. M. Mulder, and I. M. de Schepper, Physica **276-278**, 950 (2000).
[21] V. W. J. Verhoeven, I. M. de Schepper, G. Nachtegaal, A. P. M. Kentgens, E. M. Kelder, J. Schoonman, and F. M. Mulder, Phys. Rev. Lett. **86**, 4314 (2001).
[22] J. B. Goodenough, *Magnetism and the Chemical Bond* (Wiley, New York, 1963).
[23] E. J. W. Verwey and P. W. Haaymann, Physica (Utrecht) **8**, 979 (1941).
[24] Y. Liu, T. Fujiwara, H. Yukawa, and M. Morinaga, Solid State Ionics **126**, 209 (1999).
[25] H. Berg, K. Göransson, B. Noläng, and J. O. Thomas, J. Mater. Chem. **9**, 2813 (1999).
[26] D. J. Singh, Phys. Rev. B **55**, 309 (1997).
[27] M. K. Aydinol, A. F. Kohan, G. Ceder, K. Cho, and J. Joannopoulos, Phys. Rev. B **56**, 1354 (1997).
[28] S. K. Mishra and G. Ceder, Phys. Rev. B **59**, 6120 (1999).
[29] A. Van der Ven, C. Marianetti, D. Morgan, and G. Ceder, Solid State Ionics **135**, 21 (2000).
[30] J. P. Perdew, K. Burke, and M. Ernzerhof, Phys. Rev. Lett. **77**, 3865 (1996).
[31] U. von Barth and L. Hedin, J. Phys. C **5**, 1629 (1972).
[32] J. M. Wills, O. Eriksson, M. Alouani, and D. L. Price, in *Electronic Structure and Physical Properties of Solids*, edited by Hugues Dreysse (Springer Verlag, Berlin, 2000), p. 148; M. Alouani and J. M. Wills, *ibid.* p. 168; O. Eriksson and J. M. Wills, *ibid.* p. 247.
[33] D. J. Chadi and M. L. Cohen, Phys. Rev. B **8**, 5747 (1973); S. Froyen, *ibid.* **39**, 3168 (1989).
[34] P. Ravindran, A. Delin, B. Johansson, O. Eriksson, and J. M. Wills, Phys. Rev. B **59**, 1776 (1999).
[35] P. Vinet, J. H. Rose, J. Ferrante, and J. R. Smith, J. Phys.: Condens. Matter **1**, 1941 (1989).